

Article

A Distributed Vision-Based Navigation System for Khepera IV Mobile Robots

Gonzalo Farias^{1,*} , Ernesto Fabregas² , Enrique Torres¹ , Gaëtan Bricas³ , Sebastián Dormido-Canto² , and Sebastián Dormido² 

¹ Pontificia Universidad Católica de Valparaíso, Av. Brasil 2147, Valparaíso, Chile; gonzalo.farias@pucv.cl

² Departamento de Informática y Automática, Universidad Nacional de Educación a Distancia, Juan del Rosal 16, 28040 Madrid, Spain; efabregas@dia.uned.es

³ The National Institute of Electrical Engineering, Electronics, Computer Science, Fluid Mechanics & Telecommunications and Networks. 2, rue Charles Camichel, 31071 Toulouse Cedex 7, France

* Correspondence: gonzalo.farias@pucv.cl

Abstract: This work presents the development and implementation of a distributed navigation system based on computer vision. The autonomous system consists of a wheeled mobile robot with an integrated colour camera. The robot navigates through a laboratory scenario where the track and several traffic signals must be detected and recognized by using the images acquired with its on-board camera. The images are sent to a computer server that processes them and calculates the corresponding speeds of the robot using a cascade of trained classifiers. These speeds are sent back to the robot, which acts to carry out the corresponding manoeuvre. The classifier cascade should be trained before experimentation with two sets of positive and negative images. The number of images in these sets should be considered to limit the training stage time and avoid overtraining the system.

Keywords: mobile robot; vision-based navigation; cascade classifiers

1. Introduction

The current development of robotics has been influenced by the growth of NICT (New Information and Communication Technologies), which has provided the perfect scenario for the confronting of new challenges. In this context, the autonomous navigation of robots based on vision has grown considerably, showing increased interest for some years now.

This interest began some years ago, when researchers [1] and [2] presented two systems for navigation based on vision with obstacle detection and avoidance in outdoor scenarios in 1988. These works obtained very good results considering the technologies available at the time (cameras, processors, communications, etc.). Another example was published in 2002, in which the authors presented a study on the navigational vision of mobile robots spanning 20 years [3].

In this comprehensive and in-depth survey, interesting breakthroughs can be found in approaches that make a distinction between indoor and outdoor environments [4–7]. In recent years, navigation based on vision has shown renewed interest in the scientific and educational communities [8–11] because it has many practical applications in daily life.

Robots that can navigate autonomously are complex systems involving several components that have a common denominator: communication capabilities and the speed of processing and operation. These capabilities are very important because an autonomous robot must have all the necessary information available to make the right decisions at every sampling time.

Currently, it is common to find robots in the market that integrate cameras with good resolution, high processing performance and communication capabilities such as Bluetooth or WI-FI, which were

31 not available until recently; examples include the e-puck robot [12], Khepera IV [13], Pioneer 3-DX
32 [14], and TurtleBot3 [15].

33 These capabilities are important in robot vision-based navigation because robots need to acquire
34 images of their environment, process them, and make decisions to navigate through a scenario [16] and
35 [17]. In the case of robots that are not capable of performing complex tasks such as image processing,
36 these images can be acquired with a camera and sent to a server for processing. The server can answer
37 with the orders for the motors of the robot to navigate, or these orders can be calculated in the robot
38 with the results of the image processing. This introduces a delay of the network in the control loop,
39 which is an important element that must be considered in these systems. In a local WI-FI network, this
40 delay should not affect the operation of the system. The fact that the processing is done in a server
41 allows another type of hard task, such as the implementation of machine learning algorithms [18–20],
42 which may require a training stage before use.

43 In the literature, you can find some research articles related to vision-based systems using different
44 techniques. For example in [21], the authors present a system for the detection of persons using cascade
45 classifiers. Its method uses the implementation of HOG (Histogram of Oriented Gradients) feature
46 descriptor and AdaBoost algorithm with a 2D laser and a camera. In [22], the authors developed a
47 vision-based control system for the alignment of an autonomous forklift vehicle. They implemented
48 Haar feature-based cascade classifiers for detection and heavy spool pick-and-place operation. In [23],
49 the authors presented two systems for detection and classification of traffic signs in real time. The
50 first method is divided into three stages: color segmentation using a threshold, detection using SVM
51 (Support Vector Machine) and classification tree-like and Random Forest. In [24], the authors propose
52 a detection and recognition system for road warning signs with voice notification for autonomous
53 vehicles. It implements Haar feature-based cascade classifiers. In [25], the authors describe a navigation
54 system of a robot based on paths following. The method uses a combination of the detection of colours,
55 textures and lines with different classifiers.

56 As can be seen, there is a wide range of approaches to this topic. After an exhaustive analysis of
57 all mentioned works, we realized that none of them is available for laboratory practices with students,
58 which is one of our main purposes with this research.

59 This article presents a distributed vision-based autonomous navigation system with machine
60 learning in a laboratory environment. The system consists of a Khepera IV robot that acquires the
61 images and sends them to a server. On the server, a trained cascade of classifiers processes the
62 images and calculates the linear and angular velocities of the robot to navigate through the indoor
63 experimental environment built in the laboratory.

64 The main motivation for this work is that our Engineering School has implemented a platform
65 for educational and research purposes in the field of mobile robotics [26,27]. In which students can
66 experiment with their own controllers in order to incorporate these concepts in the teaching of robot
67 control. In this sense, experiments on position control, obstacle avoidance, among others, have been
68 implemented with very good results, for example [28–31].

69 Now the purpose is to use the robot's on-board camera to develop even more challenging
70 experiments that attract the students in an interactive environment. These artificial vision experiments
71 can improve the quality of the laboratory practices, which can mean a step up in the teaching-learning
72 process of mobile robot labs.

73 The main contribution of this work is to propose the use of advanced computer vision algorithms
74 to perform much more sophisticated and engaging experiments with practical mobile robot laboratories
75 for pedagogical purposes. The motivation of this is to provide much more challenging experiments for
76 the students to improve the quality of the teaching-learning process in this field. A summarized list of
77 contributions of this work is the following: 1) the incorporation of new computer vision capabilities
78 to the practical mobile robot laboratories; 2) to provide much more challenging experiments in an
79 interactive and engaging environment; 3) introduce advanced algorithms for image processing and
80 artificial intelligence techniques for teaching control of mobile robots; and 4) the experiments can

81 be tested in simulation firstly, and after that, they can be implemented in a real and easy-to-use
82 environment in a relatively fast and straightforward way.

83 The remainder of the paper is organized as follows: Section 2 presents the fundamental concepts
84 related to this article; Section 3 describes the implementation of the experiments in the laboratory;
85 Section 4 shows the results of some test experiments developed in simulation and with the platform;
86 and finally, Section 5 presents the main conclusions and future work.

87 2. Background

88 The vision-based system consists of the processing of images acquired by the on-board camera.
89 Today, you can find some software libraries to carry out this process, such as Torch3vision, VXL (Vision
90 something Libraries), JavaVIS, LIT-lib, and OpenCV (Open source Computer Vision library) [32]. After
91 some studies and tests, OpenCV was selected to carry out the image processing. It presents the most
92 complete solutions for the problems that we face processing the images acquired by the robot.

93 OpenCV is a library of functions for real-time computer vision that was developed by Intel. It
94 is free for use under an open-source license. It has interfaces for C++, Python, and Java. It is very
95 versatile because it can be compiled for Windows, Linux, Mac OS, IOS and Android. It has more than
96 2500 optimized algorithms that include machine learning, face detection, motion detection, object
97 tracking, 3D object model extraction, finding similar images in a database, augmented reality [33], etc.
98 In our case, its main drawback is that it cannot be executed on the robot. That is why we need to send
99 the images from the robot to a server to process them and calculate the orders for the robot.

100 2.1. Image Segmentation

101 Different techniques are used to obtain the features of an image. One of the most commonly used
102 techniques is segmentation, which consists of dividing the image into multiple segments (set of pixels)
103 to obtain the information from these segments (also known as super-pixels). The idea is to simplify the
104 image into something that is easier to analyse [34]. This process is commonly used to detect objects
105 and boundaries such as lines, curves, edges, corners, etc. As a result, a set of segments is obtained
106 that is determined by regions with similar characteristics such as intensity, colour or texture. The
107 simplest method in segmentation is thresholding, which can create a binary image (black/white) from
108 a colour image. If the original image is (x,y) , the segmented image is (x',y') , which is determined by the
109 threshold $U(0 < U < 255)$. This operation is defined as follows:

$$(x',y') = 255, \text{ if } (x,y) > \text{Threshold} \quad (1)$$

$$(x',y') = 0, \text{ if } (x,y) \leq \text{Threshold} \quad (2)$$

110 The value of the threshold is selected depending on the colours that must be grouped to establish,
111 for example, a difference from the background of the image. Figure 1 shows the traffic signals that will
112 be used for navigation.



Figure 1. Traffic signals that must be detected.

113 2.2. Cascade of Classifiers

114 Cascade classifiers are a concatenation of ensemble learning based on several classifiers. Each
 115 basic classifier implements the AdaBoost algorithm in a decision-tree classifier with at least 2 leaves.
 116 The information from the output of a given classifier is used as an additional input of the next classifier
 117 in the sequence [35]. All the classifiers of the cascade are trained with a set of images of the same size
 118 called "positive", which are sample views of the object to be detected and arbitrary "negative" images
 119 of the same size.

120 After the classifier is trained, it can be applied to a search window (of the same size as used during
 121 the training) to detect the object in question in the entire frame [36]. This process is repeated until
 122 at some stage the analysed segment of the image is rejected or all the stages are passed. The search
 123 window can be moved across the image to check every location for the classifier. The classifier outputs
 124 a "T" if the region is likely to show the object and "F" otherwise. In an image, the extraction of features
 125 can be obtained from several methods, including Haar, LBP and HOG. Figure 2 shows this process
 126 [37].

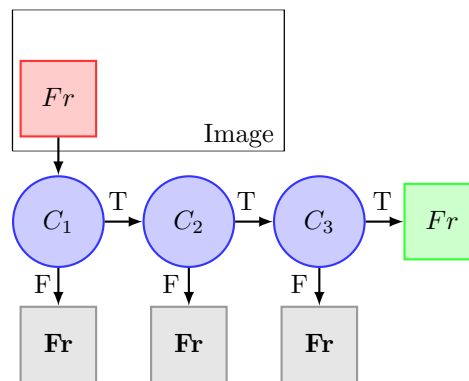


Figure 2. Applying cascade classifiers to the search window on an image.

127 The magenta circles represent the classifiers (C_1 , C_2 and C_3). The red square represents the frame
 128 of the image that is being analysed. If the object is detected, the output of all classifiers is T, and the
 129 (green square) frame represents this situation. However, if some of the classifier outputs are F, the
 130 frame is rejected (grey squares), and the object is not detected in this frame.

131 3. Implementation in the laboratory

132 3.1. Platform used

133 The implementation of the system is based on the platform developed by the authors in a previous
 134 work [26–28] with some modifications. Figure 3 shows a diagram of the platform in the laboratory.



Figure 3. Diagram of the platform used for the experiments.

135 The system is composed of Khepera IV robots that run software that grants communication and
 136 operation. The other component is a server that processes the images acquired by the Khepera IV robot
 137 and calculates the velocities to control it. As mentioned before, this software has been developed in
 138 Python and uses the OpenCV library to work with the images. The wireless communication between
 139 the robot and the system is carried out with a WI-FI router. Furthermore, a Play Station 3 USB camera
 140 is connected to the server to obtain the overhead view of the experiments in the server. This video
 141 signal is used to watch the development of the experiments by the user.

142 The setup of the platform for the experiments is the following: The dimensions of the arena are
 143 $2.0m \times 1.5m$. The dimensions of the robot Khepera IV are $140mm$ (diameter) and $58mm$ (height). The
 144 Dimensions of traffic signals are $26mm \times 26mm$. The Number of traffic signals is 8.

145 3.2. Objects detection system

146 Figure 4 shows the block diagram of the system. On the left side, the robot is represented by the
 147 green dashed line block.

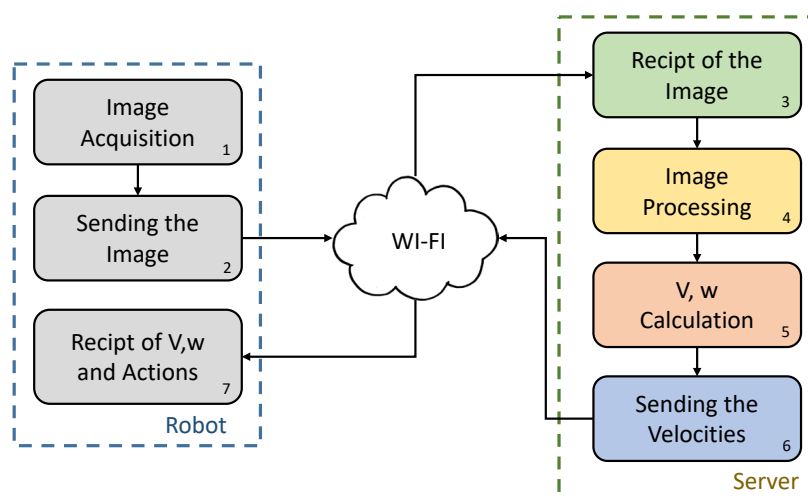


Figure 4. Block diagram of the system.

148 On the right side, the server is represented by the yellow dashed line. The system works as
 149 follows, where the numbers represent the order in which the task is executed:

- 150 • Block 1: Robot acquires the image.
- 151 • Block 2: The image is sent to the server using the WI-FI connection.
- 152 • Block 3: The image is received by the server.
- 153 • Block 4: The image is processed in the server.
- 154 • Block 5: The linear and angular velocities of the robot are updated using the results of block 4.
- 155 • Block 6: The velocities are sent to the robot through the WI-FI connection.
- 156 • Block 7: The robot receives the velocities and sends them to the motors.

157 The software that runs the robot is very simple. It consists of two main functions: 1) to acquire
 158 the image from the on-board camera and send it to the server, and 2) to receive the velocities from
 159 the server and update them in the motors. On the other hand, the software that runs at the server is
 160 more complex because it carries out more difficult tasks, including image processing. Figure 5 shows a
 161 simplified block diagram of this application. The tasks are divided into the four blocks of the server
 162 side of Figure 4.

163 The first task is to check if an image has been received. If an image is received, it is processed in
 164 the second task (Image Processing) as follows: 1) the image is read, 2) it is converted to grey-scale, 3)
 165 its resolution is obtained, 4) traffic signals are detected with the trained cascade of classifiers, and 5) if
 166 a signal is detected, its size is obtained. After that, the third task calculates the velocities of the robot

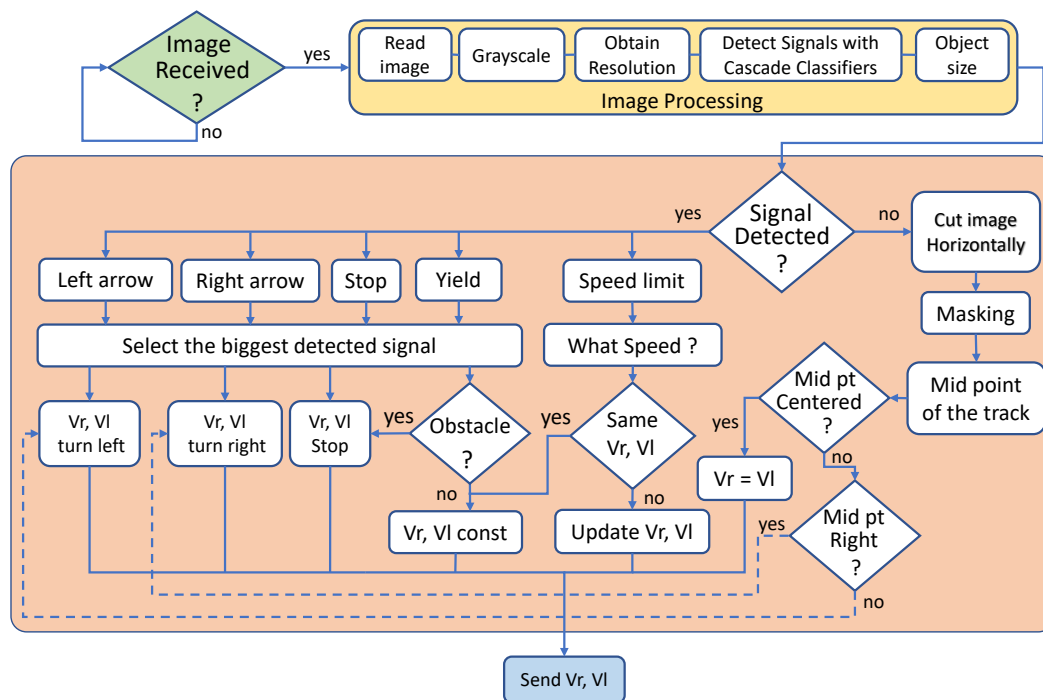


Figure 5. Block diagram of the server side application.

167 from the object detected. At the beginning of this task, the process forks into two main paths: 1) if a
 168 traffic signal is detected and 2) if the track is detected.

169 If a signal has been detected, depending on its type (left arrow, right arrow, stop, yield or speed
 170 limit), the velocities are calculated to make the corresponding action. For example: a left arrow V_L
 171 is equal to 0 and V_r is equal to 0.025, which makes the robot turns to the left. If the detected signal
 172 is a stop, both velocities are set to 0. If the signal detected is a speed limit, the signal is processed to
 173 determine the corresponding speed. On the other hand, if the object detected is a track, the image is
 174 processed by thresholding to determine if the track indicates that it is a straight path or a turn to the
 175 left or to the right. In both cases, when the velocities are calculated, they are sent to the robot and
 176 the application reverts back to the beginning to wait for other new images.

177 3.3. Implementing cascade classifiers

178 To train the classifiers, existing databases of “positive” and “negative” images can be used, or
 179 customized databases can be created. These image training sets can be created using OpenCV. In our
 180 case, the “negative” image set was created using the on-board camera of the robot.



Figure 6. Examples of negative images acquired by the robot.

181 Figure 6 shows on the left side, 4 examples of “negative” images obtained by the robot. To provide
 182 correct training, these images must not contain the object that wants to be classified as positive. The set
 183 of negative images for this experiment was composed of approximately 1400 images. Figure 6 shows
 184 on the right side, 4 examples of the positive images acquired by the robot. In this case, the object that
 185 wants to be detected is the signal of the airport, which is included in all positive images. In this case,
 186 the number of positive images was approximately 1000. With these two sets of images, the OpenCV
 187 function “training cascade” was used to carry out the training stage.

188 The selected classifiers were Haar-like with 5 stages in the cascade. A high number of classifiers
 189 in the cascade improves the classification, but the training time can increase exponentially. We selected
 190 Haar feature-based algorithm because this classifier showed encouraging performance with high
 191 success recognition rates for this experiment.

192 3.4. Code of the robot

193 As mentioned before, the programming code of the robot has been developed in Ansi C, which
 194 is the programming language that the robot uses. The following code segment shows the algorithm.
 195 Note that some lines have been omitted for space reasons.

```

196 1 #include <khepera/khepera.h>,<signal.h>;
197 2 #include <stdio.h>,<string.h>,<sys/socket.h>;
198 3 #include <arpa/inet.h>,<unistd.h>;
199 4
200 5 static knot_dev_t*$dsPic; // Robot PIC microcontroller
201 6 int main(int argc, char **$argv){
202 7 ...// Define variables and Server Socket
203 8 ...// Server Socket is listening (192.168.0.111:8080)
204 9 ...// Accept connection from an incoming client
205 10 ...// Initiate libkhepera and robot access
206 11 ...// Open robot socket, store the handle in its ptr
207 12 ...// Initialize the motors with tuned parameters
208 13
209 14 // Receive a msg from client
210 15 while((read_size=recv(client_sock ,client_msg ,4 ,0))>0){
211 16 // Execute received velocities
212 17 write(client_sock ,client_msg ,strlen(client_msg));
213 18 vLeft=client_msg[0]-'0';
214 19 vRight=client_msg[1]-'0';
215 20 printf("%i_%i_\n",vLeft ,vRight);
216 21 kh4_SetMode(kh4RegSpeedProfile ,dsPic);
217 22 kh4_set_speed (vLeft*10 ,vRight*10 ,dsPic);
218 23 close(socket_desc);
219 24 }
220 25 ... // If an erroneous msg received rise an error msg
221 26 ... // If some button is pressed program stops
222 27 }

```

223 From lines 1 to 10, the variables and some configurations are defined. The communication socket
 224 is created and connected to the server. Through this connection, the robot sends the images acquired by
 225 the camera of the robot with the MJPG-streamer application [38]. Then, the parameters of the motors
 226 of the robots are initialized. From lines 13 to 22, a message received from the computer is processed.
 227 The velocities of the robot received in the messages are sent to the motors.

228 3.5. Code of the server

229 The following code segment shows the implementation at the server side. This code has been
 230 developed with Python. An important detail is that the server reads the images acquired by the robot
 231 using the TCP connection created and the application MJPG-streamer that is running at the robot.
 232 Note that some lines have been omitted for space reasons.

```

233 1 import re ,os ,sys ,cv2 ,numpy as np
234 2 import threading ,argparse ,time ,urllib ,socket
235 3 ... # Variables and parameters definition
236 4 ... # Creating client Socket (port 8080)
237 5 ... # Loading trained cascade classifiers
238 6 while rval:

```

```

239 7 # Read the image from the robot
240 8 # Execute cascade classifiers with the image
241 9 stops=stop_csc.detMulSc(scframe,1.05,5,
242 10 0,(1,1),(500,500))
243 11 airport=airport_csc.detMulSc(scframe,1.15,
244 12 5,0,(1,1),(500,500))
245 13 rArrow=rArrow_csc.detMulSc(np.rot90(scframe,2),
246 14 1.1,5,0,(1,1),(500,500))
247 15 lArrow=lArrow_csc.detMulSc(scframe,1.1,5,0,
248 16 (1,1),(500,500))
249 17 Yield=yield_csc.detMulSc(scframe,1.1,5,0,(1,1),
250 18 (500,500))
251 19 signs=CLASSIFIER.detMulSc(scframe,1.2,5,0,(1,1),
252 20 (500,500))
253 21 ... # Depending on the detected signal
254 22 # its area is calculated
255 23 ... # Speed limits are calculated using Flann technique
256 24 # Time of action of the signal
257 25 if time.time()-time_stop<5: state="STOP"
258 26 elif time.time()-time_TurnL<5: state="TURN_LEFT"
259 27 elif time.time()-time_TurnR<5: state="TURN_RIGHT"
260 28 else: state="GO"
261 29 if state == "GO":
262 30 # Calculate the center of the track
263 31 hsvTrac=cv2.cvtColor(imagenTrac,cv2.COLOR_BGR2HSV)
264 32 low_white=np.array([65,85,150],dtype=np.uint8)
265 33 high_white=np.array([79,90,380],dtype=np.uint8)
266 34 # Creating the Mask
267 35 maskTrac=cv2.inRange(hsvTrac,low_white,high_white)
268 36 momentsTrac=cv2.moments(maskTrac)
269 37 areaTrac=momentsTrac['m00']
270 38 if (areaTrac > 200):
271 39 xTrac=int(momentsTrac['m10']/momentsTrac['m00'])
272 40 yTrac=int(momentsTrac['m01']/momentsTrac['m00'])
273 41 cv2.rectangle(imagenTrac,(xTrac,yTrac),
274 42 (xTrac+2,yTrac+2),(0,0,255),2)
275 43 # Calculate the velocities for each signal
276 44 if abs(xTrac-192/2) < 5:
277 45 v_left=int(int(lastlimit)/14),
278 46 v_right=int(int(lastlimit)/14)
279 47 elif xTrac > 144:
280 48 v_left=int(int(lastlimit)/14),
281 49 v_right=int(int(lastlimit)/56)
282 50 elif xTrac < 192/4:
283 51 v_left=int(int(lastlimit)/56),
284 52 v_right=int(int(lastlimit)/14)
285 53 # Else, turn to the right or to the left
286 54 elif xTrac > 192/2:
287 55 v_left=int(int(lastlimit)/14),
288 56 v_right=int(int(lastlimit)/28)
289 57 elif xTrac < 192/2:
290 58 v_left=int(int(lastlimit)/28),
291 59 v_right=int(int(lastlimit)/14)
292 60 cv2.imshow('Mask', maskTrac)
293 61 elif state == "SLOW":
294 62 v_left=int(int(lastlimit)/28),
295 63 v_right=int(int(lastlimit)/28)
296 64 elif state == "STOP": v_left=0, v_right=0
297 65 elif state == "WAIT": v_left=0, v_right=0
298 66 elif state == "YIELD":
299 67 v_left=int(int(lastlimit)/28),
300 68 v_right=int(int(lastlimit)/28)
301 69 elif state == "TURN_LEFT":
302 70 v_left=0, v_right=int(int(lastlimit)/14)
303 71 elif state == "TURN_RIGHT":
304 72 v_left=int(int(lastlimit)/14), v_right=0
305 73 # Velocities converted and send them to the robot
306 74 # Sending the velocities to the robot
307 75 cv2.putText(origframe,"Current_speed_limit:"
308 76 +str(lastlimit)+"km/h.",(5,20),
309 77 cv2.FONT_HERSHEY_SIMPLEX,0.45,(255,255,255),1)
310 78 cv2.imshow("preview",frame)
311 79 k=cv2.waitKey(30) & 0xff
312 80 if k == 27: break

```

313 From lines 1 to 5, certain tasks are carried out: the variables are defined; the client socket is created
314 and connected; and the trained cascade classifiers are loaded. After that, the main loop starts. From
315 lines 9 to 20, the image from the robot is obtained and conditioned. From lines 24 to 29, the cascade of
316 classifiers is applied to the obtained image. The result of this operation is that only one classifier must
317 be true. If not, the traffic signal is detected with the classifiers, which means that the track must be
318 followed. With the result of the classifiers, the velocities are calculated from lines 30 to 72. Then, the
319 velocities are sent to the robot from lines 73 to 77. Finally, the program waits for a key to finish.

320 4. Experimental Results

321 In this Section, all the tests that were carried out for the detection of objects and navigation of the
322 robot are shown. The results are represented from the detection of basic signals (arrows of the same
323 colour) to more complex signals, which are involved in the tests of the designed classifiers (presented
324 in Section 3), as well as traffic signals and new scenarios. These results reflect the efficiency of this new
325 algorithm, both simulated and with the real robot. The Section describes three experiments. The first
326 experiment shows the difficulties of detecting multiple objects by using traditional image processing.
327 The second experiment describes the advantage of the cascade classifier for recognition of several
328 traffic signals, and finally, the third experience provides the results of the implemented vision-based
329 navigation system to perform an advanced experiment in the real environment.

330 4.1. Experiment 1: Object detection by image processing

331 To initiate the proposed algorithm, a simulation of a simple scenario was performed using the
332 V-REP simulator and the Khepera IV robot model previously developed by the authors [29] and [30].
333 The experimental concept is that the robot can navigate through the arena, detecting the arrows.

334 This work is based on a previous work of the authors presented in [31]. The robot control
335 algorithm must be able to calculate the corresponding speeds that allow the robot to turn in the correct
336 direction depending on the arrow detected. For the first experiment, the arrows are of the same colour
337 to simplify the identification because, using the threshold technique, the arrows can be easily detected.
338 Figure 7 shows the configuration of this experiment on the left side. In the upper right corner of the
339 scenario, the images acquired by the on-board camera of the robot are shown in running time.

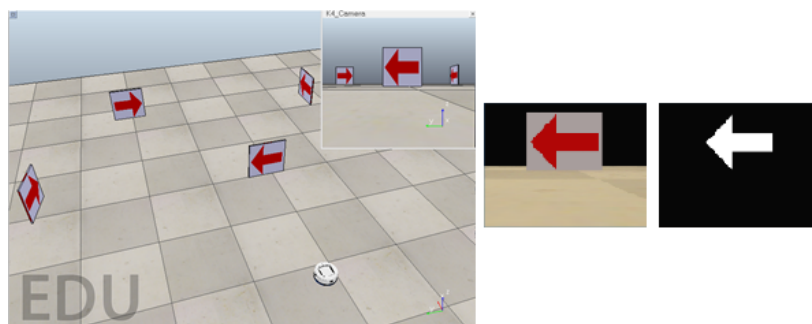


Figure 7. Experimentation detection of arrows of the same color in a simulated environment.

340 Once the image is detected by the robot in the program, red masking is performed, which only
341 displays the characteristics of the red arrow, as shown on the right side of Figure 7. The image on the
342 left is the image acquired by the robot camera, and the image on the right side is the result from the
343 red masking. The image is segmented in such a way that there is a margin where only the colour red
344 appears. In that image, there may be several arrows, so the robot determines the largest arrow, since it
345 is assumed that this arrow will be the closest to the robot and thus will have more relevance.

346 OpenCV provides multiple tools to discern the orientation of an object, including `cv.minAreaRect`,
347 `cv.fitEllipse` and `cv.fitLine`. In our case, `cv.fitLine` was used. This function provides four variables that
348 can be used to obtain two other variables called `lefty` and `righty`. In the case of arrow detection, if it is

349 oriented to the left, the value of the lefty variable is positive, and right is negative. However, if the
 350 arrow is oriented to the right, these values change their sign.

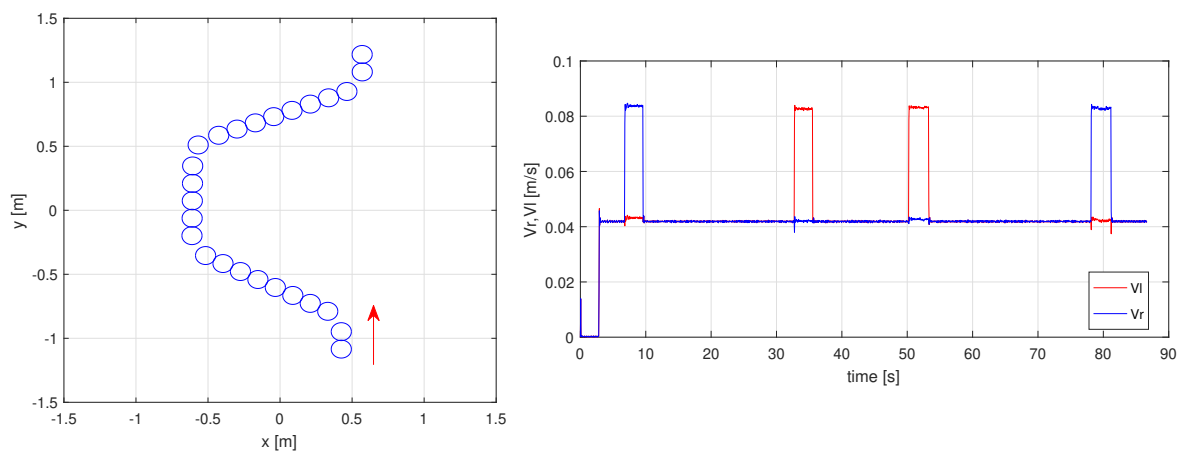


Figure 8. Trajectory of the robot and its corresponding velocities.

351 Figure 8 shows the path of the robot on the upper side, which indicates that the robot is performing
 352 autonomous behaviour. It detects the arrow direction and makes the correct decisions to turn to the
 353 right and to the left depending on each arrow. The bottom side of this figure shows the speed behaviour
 354 of each motor during the experiment. In the first stage, the speed of the right motor is greater than
 355 that of the left, so the robot makes a leftward turn. Then, the speeds are equal again. In the second
 356 stage, the speed of the left motor is greater, so the robot turns to the right. In the third stage, the robot
 357 turns to the right, and in the last stage, the robot turns to the left. In conclusion, the robot detects four
 358 arrows and affirmatively avoids them by producing an algorithm to detect and avoid arrows.

359 As in the simulated experiment, a test involving the detection of arrows was also carried out with
 360 the platform. Figure 9 shows the configuration of this experiment on the left side. The robot is near
 361 three red arrows, which are positioned at 80 cm and have an orientation of 90 degrees with respect to
 362 each other. As in the previous case, the goal of the robot is to detect these arrows and make decisions
 363 to navigate through the scenario.

364 On the right side of Figure 9, the image acquired by the robot and its corresponding masking
 365 of the red colour are shown. In the virtual experience, the cv.fitLine function was used, but in this
 366 case, the function did not provide a good result; it did not clearly detect the orientation of the arrow.
 367 Therefore, another technique was used according to the following criterion: An arrow has seven
 368 vertices, but two of them are located at the top and bottom of the image; therefore, depending on the
 369 location of those points on the x-axis, the robot can determine the orientation of the arrow.



Figure 9. Example of experimental detection of arrows of the same colour in a real environment.

370 Note that this is a previous stage of the algorithm that we want to implement. This method needs
 371 a lot of knowledge (features) about the object to be identified. That is why we have used OpenCV
 372 functions and the robot Khepera IV, to show this drawback. On the contrary, we want to implement a

373 system that is capable of detecting known objects from the training stage, and at the same time, a new
 374 object can be added to the experiment just re-training the system.

375 4.2. Experiment 2: Traffic signals detection by cascade classifier in simulation

376 After testing the system with these simple examples, the detection of more complex objects, such
 377 as traffic signals, is implemented both in simulation and with the platform. The simulation test consists
 378 of a classic example of a vehicle on a public road. The robot faces different traffic signals during its
 379 displacement. In this case, the robot must detect 6 traffic signals to reach its objective, which in this
 380 case is the airport signal. Figure 10 shows the configuration of this experiment in the V-REP simulator.
 381 On the right side of the figure, the image acquired by the robot shows this signal.

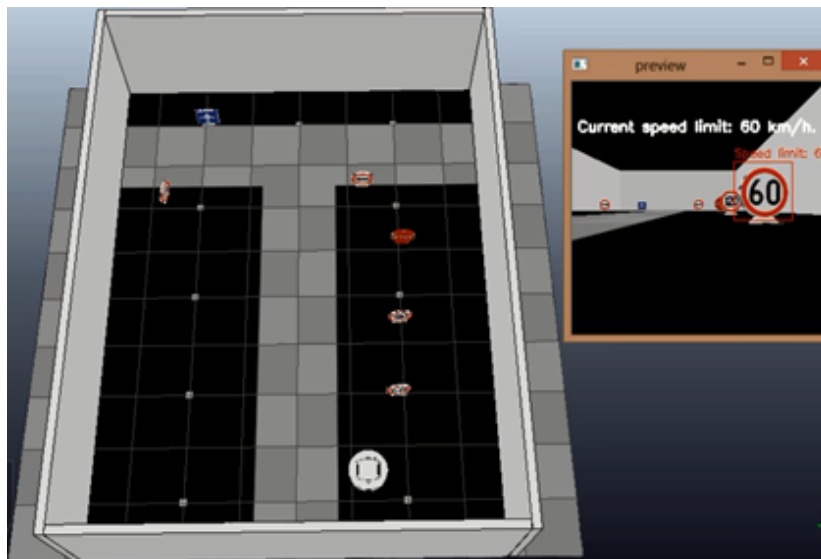


Figure 10. Experimentation detection of traffic signals in simulation.

382 At the beginning of the experiment, the robot starts to advance linearly with both velocities at
 383 0.0418 [m/s]. When it detects the first signal (60), it decreases both velocities by approximately 0.025
 384 [m/s] over 4.5 [s], which means that it continues advancing but with less speed. Then, it detects the
 385 120 speed limit signal, and it increases both velocities to double the previous value to 0.05 [m/s] over
 386 9.7 [s] and continues with a straight trajectory. After that, the next signal detected is a stop, which
 387 makes the robot decrease its speeds until reaching 0 [m/s] over 2.15 [s].

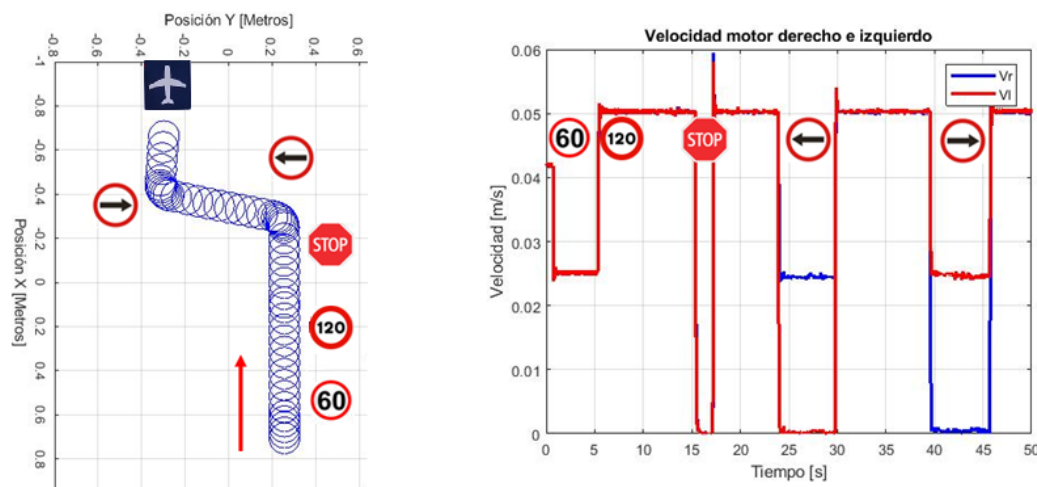


Figure 11. Position of the robot during the experiment and its corresponding velocities.

388 The next detected signal is an arrow that indicates that the robot must turn to the left. This makes
 389 the left wheel velocity 0 [m/s] and the right 0.025 [m/s] over 5.85 [s]. Then, the next signal is detected
 390 by another arrow but indicates turning to the right. This makes the right velocity decrease to 0 [m/s]
 391 and the left velocity increase to 0.025 [m/s]. At this point, the last signal (airport) is detected, and the
 392 robot stops. Figure 11 shows the position of the robot during this experiment with its corresponding
 393 traffic signals in the trajectory on the upper side. On the bottom side, the corresponding velocities of
 394 this experiment are shown.

395 The cascade classifier was trained by following the methodology described in Section 3.3. The
 396 training time to build the classifier for the eight traffic signals was about 5 hours.

397 4.3. Experiment 3: Vision-based navigation in the real laboratory

398 In this experiment, the vision-based navigation system is implemented in the real environment to
 399 detect and classify several traffic signals. Based on the previous results, it was added a white track to
 400 the real laboratory in order to aid navigation of the robot. To this end, the images of the track acquired
 401 by the on-board camera are also sent to the server and processed by the threshold technique as in
 402 [39]. Finally, the robot must move over the track by using the traffic signals. Figure 12 shows the track
 403 added to the arena.

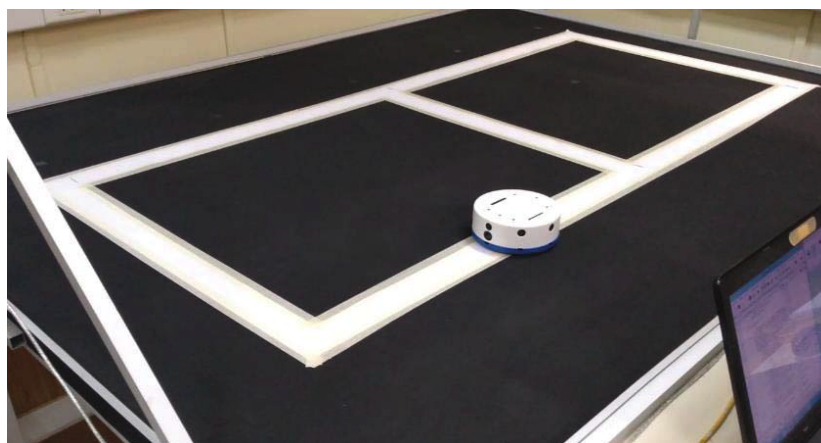


Figure 12. Track added to the platform to help the navigation.

404 Figure 13 shows three subfigures; in each, the left side shows the image acquired by the on-board
 405 camera of the robot, and the right side shows the result of the threshold technique applied to this
 406 image. The result of the first image is that the robot must turn to the left. The result of the second
 407 image is that the robot must turn to the right. The result of the last image is that the robot must go
 408 straight. In this way, the robot will take actions based on both the traffic signals and the track.



Figure 13. Experimental detection of tracks in a real environment.

409 After these modifications and tests, a more complex circuit was implemented with 13 traffic
 410 signals, including the logo of our university, a McDonald's symbol and the airport symbol. Figure 14
 411 shows the configuration of this experiment in the laboratory with the platform.

412 The experiment begins with the robot located above the white track to guide its path. The first
 413 manoeuvre of the robot is to turn to the right. This order is calculated based on the image of the track
 414 obtained by the robot. After that, the next signal detected is a stop, which is applied to reduce the
 415 speed of the robot. The next step is a straight advance based on the track until a turn to the right is



Figure 14. Experimental detection of traffic signals in a real environment.

416 executed, also based on track information. After that, the robot advances straight along the track until
 417 a right turn arrow appears, and it continues to the target (McDonald symbol), by following the track
 418 and traffic signals.

419 The main metric for object detection corresponds to a fraction of the frames with a successful
 420 recognition of the traffic signals. In the experiment shown in Figure 14, the detection rates for each
 421 signal are the following: 100% for right and left arrows, 72% for the stop signal and 88% for the airport
 422 signal, 62% for the 60-speed limit and 85% for the 100-speed limit signals.

423 The upper side of Figure 15 shows the trajectory followed by the robot in the circuit; the bottom
 424 side shows the corresponding velocities during the experiment. In the first 195 seconds, the speeds of
 425 the motors range between 0 and 0.02 [m/s] since their maximum speed is equivalent to 100 [km/h].
 426 Depending on the speed limit signal, the speeds of the motors increase or decrease. Thus, when the
 427 speed limit signal is 60, the maximum motor speed decreases to 0.014 [m/s], and when the speed limit
 428 signal is 120, the maximum velocity increases to 0.027 [m/s]. The total duration of the trajectory is 300
 429 [s].

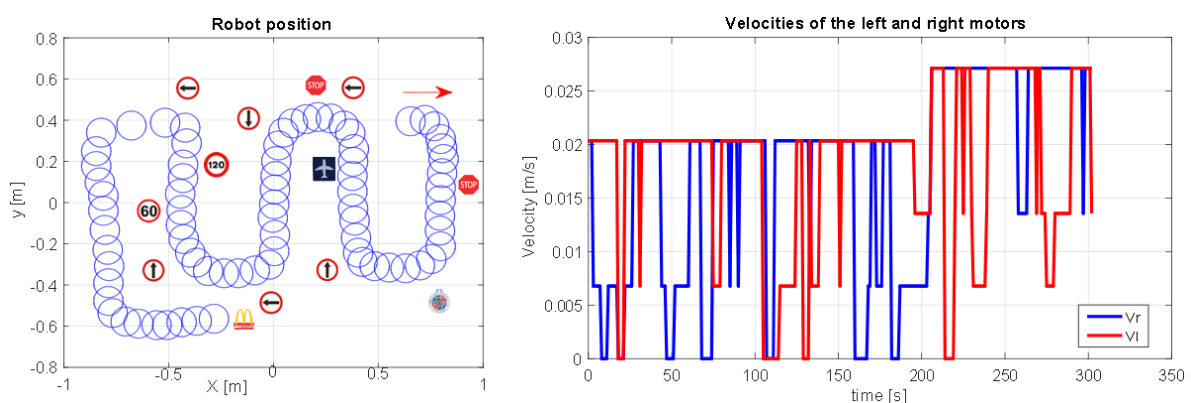


Figure 15. Position and velocities of the robot during the experiment.

430 Finally note that there are three main processing times in the real environment: Acquisition and
 431 sent of the image captured by the robot's camera to the server (approximately between 100ms and
 432 150ms), the classification time of the cascade algorithm (in average about 30ms), and the time required
 433 to send the command signals to the Khepera robot from the server (around 10ms). Thus, the total

434 processing time for the vision-based navigation system is about 200ms, which is equivalent to 4mm at
435 the maximum speed of the robot (27mm/s).

436 5. Conclusions

437 This work presented a vision-based system in a laboratory environment. The robot used for
438 the implementation is a Khepera IV, which presents high performance for this kind of application.
439 However, the robot cannot carry out image processing on-board to navigate through the scenario by
440 analysing complex information such as traffic signals.

441 After some simulations and tests, a server was added to the system to implement image processing.
442 In this way, the system was transformed into a distributed system, where the image acquired by the
443 robot is sent to the server using a WI-FI network configured for the experiments. In the server, the
444 image is processed using different image algorithms. To perform a more complex analysis of the
445 scenario, a cascade of classifiers has been developed to interpret several traffic signals (speed limits,
446 yield signal, stop signal, airport, etc.). The analysis of the traffic signals allows the robot to compute
447 the corresponding motor speeds. The calculated velocities are then sent to the robot to make the
448 corresponding manoeuvre at each sample time. To complement the scenario, multiple tracks are added
449 where the robot can move. The image of a track is also processed by the server.

450 The performance of the system is highly encouraging. The communication process is fast enough
451 to acquire the image, send it to the server and move the robot according to the velocities received. The
452 hardest task is training the cascade of classifiers. The time can increase exponentially depending on
453 the number of images used in the training. This aspect must be considered when building a similar
454 system that includes many more signals. Future work will include the implementation of different
455 classifiers with other image processing algorithms in the server and the addition of more than one
456 robot to perform exploring and collaboration mapping.

457 **Author Contributions:** E. Torres, G. Bricas and E. Fabregas designed and developed the experiments in simulation
458 and in the real environment. E. Torres and E. Fabregas collaborated in the development of the platform and
459 wrote the manuscript. G. Farias, S. Dormido-Canto and S. Dormido performed the theoretical conception, formal
460 analysis, resources, validation, founding and planning of the system.

461 **Funding:** This work has been funded by the Chilean Ministry of Education under the Project FONDECYT
462 Regular 1191188, the Spanish Ministry of Economy and Competitiveness under Projects ENE2015-64914-C3-2-R
463 and RTI2018-094665-B-I00, and the Spanish Ministry of Science and Innovation under the Project
464 PID2019-108377RB-C32.

465 References

- 466 1. C. Thorpe, M.H. Hebert, T. Kanade and S.A. Shafer, "Vision and navigation for the Carnegie-Mellon Navlab",
467 *IEEE Transactions on Pattern Analysis and Machine Intelligence*, vol. 10, no. 3, pp. 362-373, 1988.
- 468 2. M. A. Turk, D.G. Morgenthaler, K.D. Gremban and M. Marra, "VITS-a vision system for autonomous land
469 vehicle navigation", *IEEE Transactions on Pattern Analysis and Machine Intelligence*, vol. 10, no. 3, pp. 342-361,
470 1988.
- 471 3. G.N. Desouza and A.C. Kak, "Vision for mobile robot navigation: a survey", *IEEE Transactions on Pattern
472 Analysis and Machine Intelligence*, vol. 24, no. 2, pp. 237-267, 2002.
- 473 4. N.J. Nilsson, Shakey the Robot, Technical Report 323, SRI AI International Menlo Park, 1984.
- 474 5. D.A. Pomerleau, "ALVINN: An Autonomous Land Vehicle in a Neural Network", Technical Report, Carnegie
475 Mellon Univ., 1989.
- 476 6. P. Pan, D.J. Pack, A. Kosaka, A.C. Kak, "FUZZY-NAV: a vision-based robot navigation architecture using
477 fuzzy inference for uncertainty-reasoning", World Congress on Neural Networks, pp. 602-607, 1995.
- 478 7. D. Kim, R. Nevatia, "Recognition and localization of generic objects for indoor navigation using
479 functionality", *Image and Vision Computing*, no.16, vol. 11, pp. 729-43, 1998.
- 480 8. J. Gaspar, N. Winters and J. Santos-Victor, "Vision-based navigation and environmental representations with
481 an omnidirectional camera", *IEEE Trans on Robotics and Automation*, 16, pp. 890-898, 2000.

- 482 9. C. Lee and D. Kim, "Visual Homing Navigation With Haar-Like Features in the Snapshot", *IEEE Access*, vol.
483 6, pp. 33666-33681, 2018.
- 484 10. U. Witkowski, P. Bolte and J. Sitte, "Learning Vision Based Navigation with a Smartphone Mobile Robot",
485 IEEE/ASME International Conference on Advanced Intelligent Mechatronics, Auckland, pp. 1216-1221,
486 2018.
- 487 11. E. Garcia-Fidalgo, A. Ortiz, "Vision-based topological mapping and localization methods: A survey", *Robotics
488 and Autonomous Systems*, vol. 64, pp. 1-20, 2015.
- 489 12. A. G. Millard, R. A. Joyce, J. A. Hilder, C. Fleseriu, L. Newbrook, W. Li, McDaid, and D.M. Halliday, "The
490 pi-puck extension board: a raspberry pi interface for the e-puck robot platform", In IEEE/RSJ International
491 Conference on Intelligent Robots and Systems, pp. 741-748, 2017.
- 492 13. KTeam. Khepera IV User Manual, 2018. Available online: <http://ftp.k-team.com/KheperaIV/UserManual/>
- 493 14. Adept Technology, Inc. Pioneer 3-DX User Manual, 2018.
- 494 15. Robotis, Inc. Turtlebot3 User Manual, 2019. Available online:
495 <http://emanual.robotis.com/docs/en/platform/turtlebot3/overview/>
- 496 16. F.A.X. Da Mota, M.X. Rocha, J.J.P.C. Rodrigues, V.H.C. De Albuquerque and A.R. De Alexandria,
497 "Localization and Navigation for Autonomous Mobile Robots Using Petri Nets in Indoor Environments",
498 *IEEE Access*, vol. 6, pp. 31665-31676, 2018.
- 499 17. X. Gao et al., "Review of Wheeled Mobile Robots' Navigation Problems and Application Prospects in
500 Agriculture," in *IEEE Access*, vol. 6, pp. 49248-49268, 2018.
- 501 18. S. Hsu, S. Chan, P. Wu, K. Xiao and L. Fu, "Distributed Deep Reinforcement Learning based Indoor Visual
502 Navigation", IEEE/RSJ International Conference on Intelligent Robots and Systems (IROS), Madrid, pp.
503 2532-2537, 2018.
- 504 19. A. Giusti et al., "A Machine Learning Approach to Visual Perception of Forest Trails for Mobile Robots",
505 *IEEE Robotics and Automation Letters*, vol. 1, no. 2, pp. 661-667, 2016.
- 506 20. A. Mosavi, A. R. Varkonyi-Koczy, "Integration of machine learning and optimization for robot learning",
507 *Recent Global Research and Education: Technological Challenges*, pp. 349-355, 2017.
- 508 21. M. Lakrouf, L. Stanislas, D. Michel, A. Nouara, "Moving obstacles detection and camera pointing for mobile
509 robot applications," In Proceedings of the 3rd International Conference on Mechatronics and Robotics
510 Engineering, pp. 57-62, 2017.
- 511 22. A. Irawan, M. Yaacob, F. Azman, M. Daud, A. Razali y S. Ali, "Vision-based Alignment Control for Mini
512 Forklift System in Confine Area Operation," International Symposium on Agent, Multi-Agent Systems and
513 Robotics, pp. 1-6, 2018.
- 514 23. F. Zaklouta y B. Stanciulescu, "Real-time traffic sign recognition in three stages," *Robotics and autonomous
515 systems*, vol. 62, no. 1, pp. 16-24, 2014.
- 516 24. G. Archana, S. Thejas, S. Ramani, S. Iyengar, "Image Processing Approaches for Autonomous Navigation
517 of Terrestrial Vehicles in Low Illumination," 2nd International Conference On Emerging Computation and
518 Information Technologies, pp. 16, 2017.
- 519 25. H. Zhang, D. Hernandez, Z. Su y B. Su, "A Low Cost Vision-Based Road-Following System for Mobile
520 Robots," *Applied Sciences*, vol. 8, no. 9, p. 1635, 2018.
- 521 26. G. Farias, E. Fabregas, E. Peralta, H. Vargas, S. Dormido-Canto and S. Dormido, "Development of an
522 Easy-to-Use Multi-Agent Platform for Teaching Mobile Robotics", *IEEE Access*, vol. 7, pp. 55885-55897, 2109.
- 523 27. E. Fabregas, G. Farias, E. Peralta, J. Sanchez, S. Dormido, "Two Mobile Robots Platforms for Experimentation:
524 Comparison and Synthesis", International Conference on Informatics in Control, Madrid, Spain, 2017.
- 525 28. G. Farias, E. Fabregas, E. Peralta, H. Vargas, G. Hermosilla, G. Garcia, S. Dormido, "A neural network
526 approach for building an obstacle detection model by fusion of proximity sensors data", *Sensors*, vol. 18, no.
527 3, pp. 1-18, 2018.
- 528 29. E. Peralta, E. Fabregas, G. Farias, H. Vargas, S. Dormido, "Development of a Khepera IV Library for the
529 V-REP Simulator", *IFAC-PapersOnLine*, vol. 49, no. 6, pp. 81-86, 2016.
- 530 30. G. Farias, E. Fabregas, E. Peralta, E. Torres, S. Dormido, "A Khepera IV library for robotic control education
531 using V-REP", *IFAC-PapersOnLine*, no. 50, vol. 1, pp. 9150-9155, 2017.
- 532 31. G. Farias, E. Torres, E. Fabregas, H. Vargas, S. Dormido-Canto and S. Dormido, "Navigation control of the
533 Khepera IV model with OpenCV in V-REP simulator", IEEE International Conference on Automation/XXIII
534 Congress of the Chilean Association of Automatic Control (ICA-ACCA), Concepción, Chile, pp. 1-6, 2018.

- 535 32. Pulli, Kari, et al. "Real-time computer vision with OpenCV", *Communications of the ACM*, no. 55, vol.6, pp.
536 61-69, 2012.
- 537 33. Team OpenCV Developers. OpenCV, 2018. [online]. Available: <https://opencv.org/>
- 538 34. H. Kim et al., "Vision-Based Real-Time Obstacle Segmentation Algorithm for Autonomous Surface Vehicle",
539 *IEEE Access*, vol. 7, pp. 179420-179428, 2019.
- 540 35. L. Huitao, "Optimization design of cascade classifiers", IEEE Computer Society Conference on Computer
541 Vision and Pattern Recognition (CVPR'05), San Diego, CA, USA, pp. 480-485, vol. 1, 2005.
- 542 36. S.B. Kotsiantis, I. Zaharakis, and P. Pintelas, "Supervised machine learning: A review of classification
543 techniques", *Emerging artificial intelligence applications in computer engineering*, no. 160, pp. 3-24, 2007.
- 544 37. P. Viola, and M. Jones, "Rapid object detection using a boosted cascade of simple features", Proceedings of
545 the IEEE Computer Society Conference on Computer Vision and Pattern Recognition, Kauai, HI, USA, 2001.
- 546 38. S.Y. Chen, Y.H. Huang, "Research and application of open source video server MJPG-streamer", *Electronic
547 Design Engineering*, no. 5, pp. 172-176, 2012.
- 548 39. K. Lu, J. Li, X. An, H. He, "Vision sensor-based road detection for field robot navigation", *Sensors*, vol. 15, no.
549 11, pp. 29594-29617, 2015.

550 **Sample Availability:** Samples of the compounds are available from the authors.